

ORION

NEXT GENERATION WIDE-FIELD IMAGER FOR THE HUBBLE SPACE TELESCOPE

Comments to the *HST-JWST Transition Plan Review Panel*

J. MORSE (ARIZONA STATE U.),
R. WOODRUFF (LOCKHEED-MARTIN),
P. SCOWEN, J. HESTER, R. WINDHORST,
S. ODEWAHN, R. JANSEN (ARIZONA STATE U.),
T. LAUER (NOAO), A. RIESS (STSCI),
P. HARTIGAN (RICE U.),
R. KENNICUTT (U. ARIZONA),
E. CHENG (CONCEPTUAL ANALYTICS),
B. DRAKE (MEGA ENGINEERING)

24 JULY 2003

Data! data! data! I can't make bricks without clay. – Sherlock Holmes, The Adventure of the Copper Beeches.

1. INTRODUCTION

ORION is an ultra-wide-field imager concept for the *Hubble Space Telescope (HST)*. The camera is truly panchromatic, covering 200 – 1700 nm, with a >60 square-arcmin field-of-view (FOV) that is approximately six times larger than the ACS Wide Field Camera and eight times larger than the UVIS channel of WFC3. A dichroic filter is employed to split the optical beam into blue and red channels, allowing simultaneous observing in two bandpasses. The blue channel observes from the near-UV through visible wavelengths, while the red channel observes red and near-infrared wavelengths. ORION occupies an FGS instrument bay and provides fine guiding capability. It is partially based on the Ultra Wide-Field Imager (UWFI) concept that was included in the documentation that NASA provided to the *HST Post-SM4 Scientific Review Panel* (Black committee). (Some of the contributors to the UWFI report are also contributors here.)

This document provides an overview of the scientific potential of an ultra-wide-field imaging capability for *HST*, along with a possible implementation that we would propose if a Servicing Mission 5 (SM5) instrumentation Announcement of Opportunity (AO) were offered by NASA. The science topics are treated only briefly below, recognizing that the Panel is generally familiar with the underlying science issues and that other documents (e.g., “*Science with the Hubble Space Telescope in the Next Decade: the Case for an Extended Mission*” by Fall et al.) are available that discuss some of the same themes in more detail.

We provide an instrument description and performance overview in Sec. 2, a scientific

rationale in Sec. 3, and compare the concept to a MIDEX implementation in Sec. 4.

2. INSTRUMENT DESCRIPTION

2.1 HST-ORION Discovery Space

The advent of *HST* and subsequent instrumentation upgrades during the past decade have shown unequivocally that order-of-magnitude improvements in capability lead to new discoveries and rapid progress in many important fields spanning the complete range of NASA science themes, from Solar System exploration to cosmology. Considering the post-SM4 instrument complement and surveying future planned NASA missions and ground-based facilities, there remain several regions of parameter space where *HST* performance could remain unrivaled at the end of this decade if new instrumentation were enabled. In particular, the ORION camera exploits the following *HST* capabilities to achieve unprecedented performance that cannot be duplicated by any currently planned NASA mission or ground-based telescope in the post-SM5 time-frame:

- Large aperture in space with diffraction limited performance (using corrective optics)
- Stable PSF over a large field of view
- Access to UV wavelengths
- Low sky backgrounds from the UV to the near-IR
- Exquisite pointing control

ORION achieves order-of-magnitude performance gains over post-SM4 imaging capabilities by offering a field-of-view eight times larger than WFC3 and simultaneous observing in two bandpasses (Discovery Power $\approx 16\times$ WFC3). It occupies a radial FGS bay, where the largest contiguous FOV aboard *HST* is available, and includes two sensors (FGS A and B) for guiding functions. The pixel scale at the detectors is 0.1". The footprint of the ORION FOV is depicted in **Figure 2.1**. The

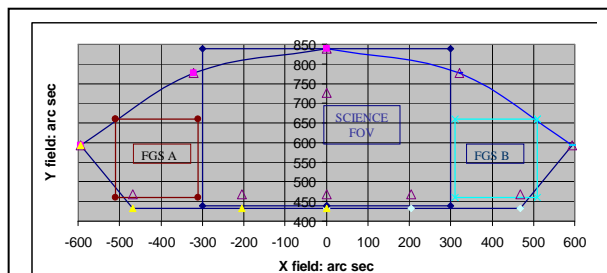


Figure 2.1: Concept for the ORION field-of-view configured in an FGS bay. The science field lies in the middle and is flanked by two guide sensors (FGS A and B). The X, Y field sizes are indicated.

4k×6k pixel science mosaic in the middle is flanked by the FGS A and B sensors. There is some vignetting of the science mosaics along the top (outer rim) of the FOV, which may be mitigated in future design iterations. The available science FOV in the current configuration is ~60 square-arcmin. A dichroic filter allows simultaneous observations over the science FOV in UV/visible and red/near-IR channels.

We provide two example benchmarks for the survey capability enabled by ORION. The first is a visual aid in **Figure 2.2** showing how virtually all of M31 can be covered in just 88 pointings. One can quickly discern the potential high impact of such an imager for achieving wide sky coverage that has thus far been impractical (or at least rare) with previous *HST* cameras.

The second comparison we provide is to the 590-orbit Cycle 12 Treasury Program by Scoville et al., called *The COSMOS 2-Degree ACS Survey*. In 4×500s exposures (1 orbit) per pointing with the ACS/WFC, the survey reaches $S/N = 10$ for point sources with $V = 27$ in the F814W filter. ORION could cover the same 2 sq-degree survey field in ~120 orbits *and* simultaneously provide V and I band images. Alternatively, in the same 590 orbits, ORION could either cover ~10 sq-degrees in two bands to the same depth, or could penetrate ~2 mags deeper in the original survey.

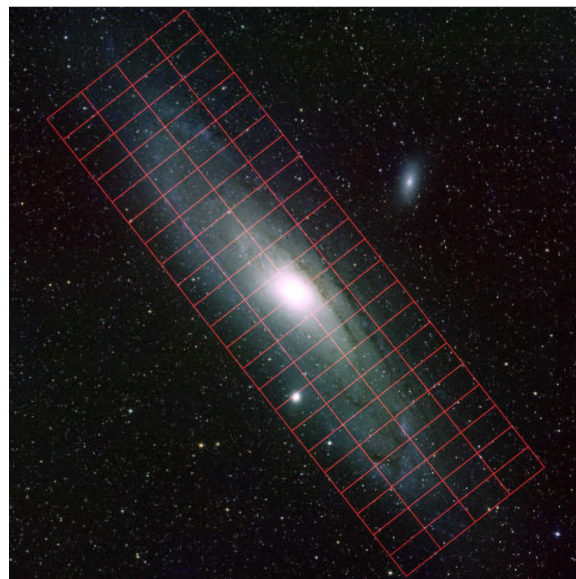


Figure 2.2: ORION could survey all of M31 in two bandpasses in just 88 pointings, demonstrating the potential for accomplishing very wide-field surveys in practical time allocations.

2.2 Technical Description

ORION is partially based on the Ultra-Wide-Field Imager (UWFI) concept (and an alternate version called HUF1) that was conceived to provide the maximum FOV allowable and practical by *HST*. ORION has a smaller FOV than UWFI, but uses a dichroic filter to double the observing efficiency.

The ORION optical design corrects a large portion of the outer *HST* FOV sampled by a Fine Guidance Sensor (FGS) “pickle”. We use a reflective optical relay (pick-off mirror or POM) to feed large detector arrays without interfering with the fields of other *HST* science instruments. The reflective relay, when combined with the *HST* OTA, nulls field curvature at the detectors, ensuring wide spectral coverage and eliminating ghosting and interface problems that a refractive field flattener would introduce. The camera uses a three-mirror relay to achieve a corrected usable FOV of ~60 square-arcminutes with an image scale of 0.1"/pixel. A long-wave pass dichroic

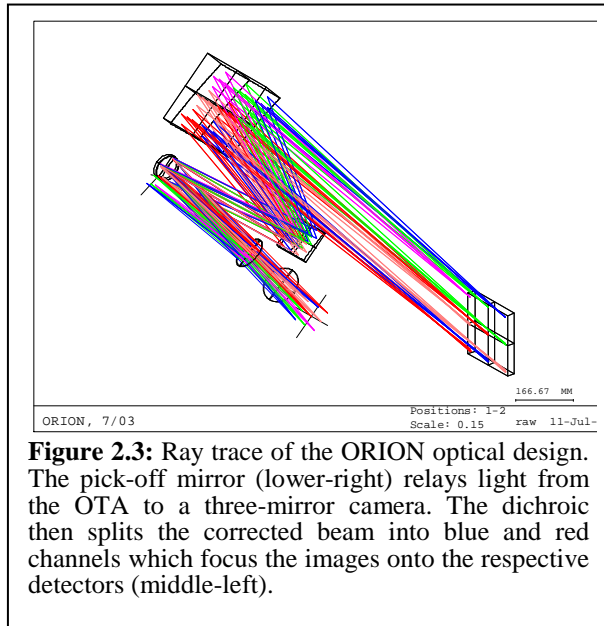


Figure 2.3: Ray trace of the ORION optical design. The pick-off mirror (lower-right) relays light from the OTA to a three-mirror camera. The dichroic then splits the corrected beam into blue and red channels which focus the images onto the respective detectors (middle-left).

filter simultaneously presents the full FOV to each of two focal plane arrays (FPAs): a UV/visible FPA covering 200 to ~600 nm and a red/near-IR FPA covering ~600 to 1700 nm. Each FPA is comprised of a 4k×6k mosaic of six 2k×2k sensors, optimized for performance in the relevant wavelength range.

The nominal design is diffraction-limited over the entire FOV at a wavelength of 520 nm. The mirrors are off-axis segments of general aspheres. They can be manufactured using technology demonstrated on previous *HST* science instruments. The dichroic filter will be designed with a scientifically optimal cut-on wavelength. All wavelengths redward (blueward) of this wavelength transmit (reflect) to the appropriate FPA. Eight filters are available in each channel. The red bandpass filters are tilted to correct lateral color introduced by the dichroic in transmission. Tilts and physical separation from the FPAs mitigate ghost reflections reaching the FPA. **Figure 2.3** shows a ray trace of the instrument from the POM to the FPAs. **Figure 2.4** shows ORION packaged in a radial FGS enclosure with key elements labeled.

Detectors. We baseline Si detectors for the UV/visible channel and HgCdTe with 1.7 μm long wavelength cut-off for the red/near-IR

channel. Both detector types are available from Rockwell Scientific in three-edge buttable 2048×2048 format mounted on a Hawaii-2RG readout. (This is the same readout as will be used for the *JWST* NIRCcam detectors.) The AR coatings will be optimized for the wavelength range served by each detector type. Each FPA is cooled by TECs and passive radiators to reduce dark current. Heat pipes strap the FPAs to *HST* radiators.

Rockwell has measured $\text{QE} > 50\%$ down to 200 nm for their Si CMOS detectors using a UV-optimized AR coating, with $\text{QE} > 70\%$ into the visible. They have measured read noise as low as 6 $\text{e}^-/\text{pixel rms CDS}$ and typically can meet $<10 \text{ e}^-/\text{pixel rms CDS}$. The dark current rates, however, have been measured at $\sim 0.5 \text{ e}^-/\text{pixel/sec}$ at 150 °K, about an order of magnitude higher than what is now being achieved with HgCdTe devices, such as the WFC3 IR channel detector. Some improvement to $<0.1 \text{ e}^-/\text{pixel/sec}$ at 150 °K (or warmer) would be desirable to take advantage of the low-background conditions. CCDs operating at $\sim 183 \text{ °K}$ (-90 °C) represent an alternate detector technology for the UV/visible channel. The implementation could be similar to the WFC3 UVIS CCD detectors (with a third 2k×4k chip), though this would introduce a separate type of readout electronics, and would lose the functionality of the H-2RG multiplexer. CCDs would also be susceptible to radiation damage and CTE degradation, however this may be less of a concern with a limited duration mission.

The red/near-IR channel detectors will be 1.7 μm HgCdTe operating at $\sim 150 \text{ °K}$, similar to the WFC3 IR channel detector but in the 2048×2048 H-2RG format. In order to maintain roughly equal numbers of filters in the two channels, the HgCdTe detectors would need to be sensitive down to $\sim 0.6 \mu\text{m}$, which can be accomplished by thinning the CdZnTe substrate. (Rockwell has demonstrated this technique as part of the *JWST* NIRCcam detector development.)

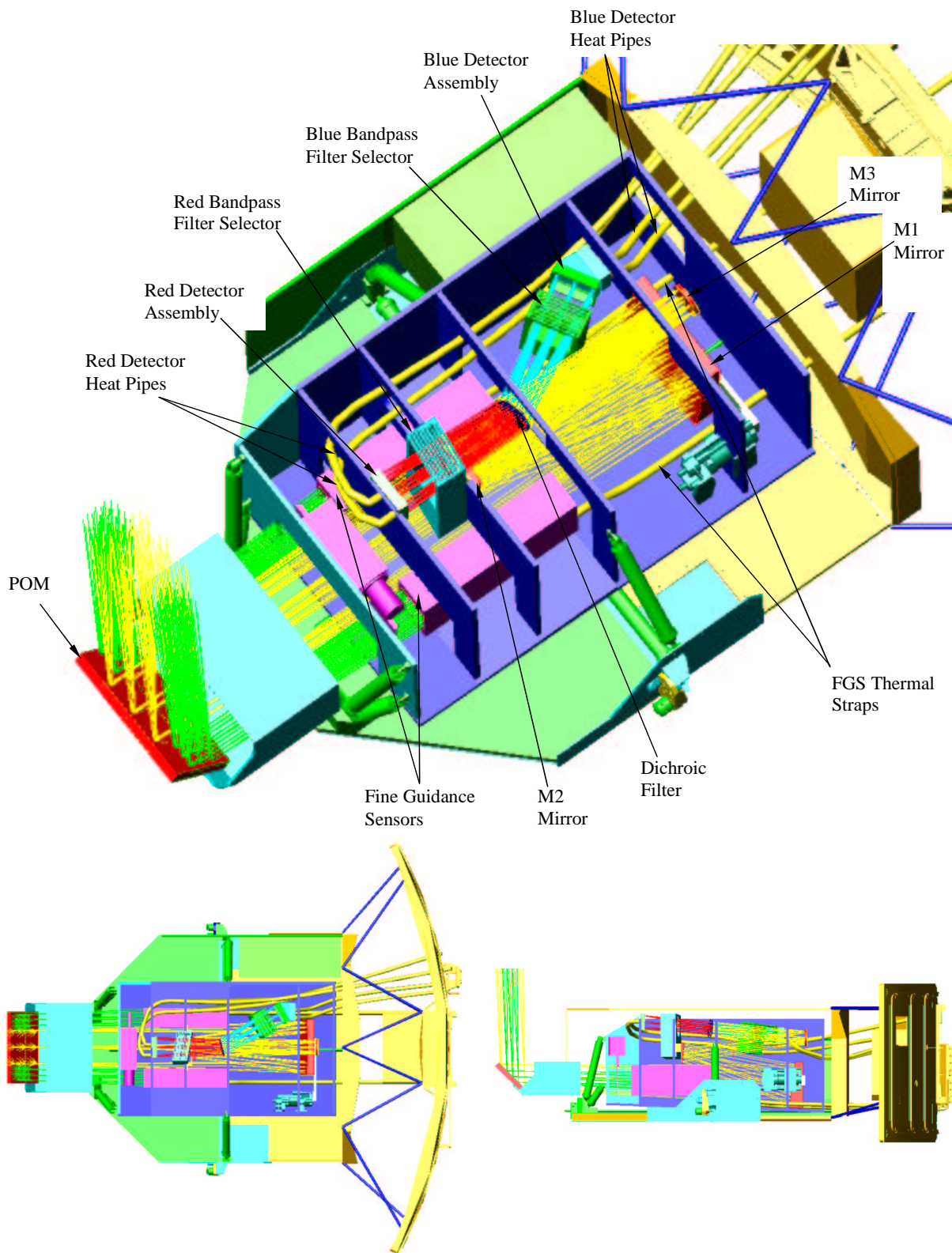


Figure 2.4: The ORION camera packaged in a radial FGS enclosure. The POM relays light from the *HST* OTA to a three-mirror (M1, M2, M3) camera. The M1 mirror provides tip/tilt and focus adjustment. A dichroic filter splits the beam into blue and red channels. The light in each channel passes through a filter selector before being focused onto the FPA. Two guide sensor assemblies bracket the science FOV. Heat pipes to the FPAs provide thermal control. Electronics boxes sit outside the optical bench assembly behind thermal standoffs.

Guiding. The Black committee expressed concern about the loss of an FGS when commenting on the UWFI concept. Operating with only two FGSs would likely limit the schedulability of some science observations, especially those with orientation constraints, and would remove redundancy for *HST* attitude and roll control in the event one of the remaining two FGSs were to fail. ORION contains two fine guidance arrays (FGS A and B) that bracket the science field, each with an 11 sq-arcmin FOV. Fixed optics placed in front of the FGS arrays correct the image and define the bandpass. The H-2RG multiplexer allows rapid readout of a small postage-stamp array that would isolate a guide star and provide feedback for pointing control, similar to the methodology to be employed on *JWST*. The information from the array could be processed for compatibility with the normal FGS error signal and relayed to the *HST* attitude control system. Although this guiding capability requires development beyond the science camera, it ensures redundancy for *HST* pointing control. (It is even possible that improved sensitivity of the ORION guiding arrays will *add* to the *HST* scheduling flexibility, though this needs further analysis.) One might also view this guiding implementation as a technological pathfinder for *JWST* fine guiding, which would otherwise be untested at the exquisite levels *JWST* requires.

Filters. We baseline 8 filters per channel for ORION. Additional filters could conceivably be included but the following satisfy the core science requirements outlined in Sec. 3. A strawman set for the blue channel filters would include UV (F225W), *u* (F336W), *b* (F438W), and *v* (F550W) broad and Mg II $\lambda\lambda 2800$ (F280N), [O II] $\lambda\lambda 3727$ (F373N), H β (F486N), and [O III] $\lambda 5007$ (F501N) narrow bandpasses. We note that a dichroic split at ~ 600 nm should help to control red leaks in the blue channel filters. The red channel filters would include *r* (F625W), *i* (F775W), *z* (F950W), *J* (F1250W), and *H* (F1600W)

broad and H α (F656N), [S II] $\lambda\lambda 6724$ (F673N), and [Fe II] $\lambda 16435$ (F1644N) narrow bandpasses. (The exact characteristics of the *v* and *r* bandpasses will depend on the adopted location of the dichroic wavelength split.)

We do not currently include grism modes in either ORION channel, since they would be available on ACS or WFC3. However, the possibility remains for including such optics.

Data handling. The FPA in each channel has 50% more pixels than the 4k \times 4k CCD mosaics of the ACS/WFC or WFC3/UVIS. Each ORION exposure would thus generate 3 times the data volume of a single exposure with either of these instruments. (Data compression techniques can essentially eliminate this disparity.) In addition, the FGS bays are not configured to dump data to the normal *HST* data handling system that serves the other science instruments. ORION would therefore need to include its own capabilities for data storage, data processing, and possibly data transmission. In principle, this is no different than what would be required for an imager being constructed for an Explorer mission, and developing the hardware and software for efficient data storage, processing, and compression is not particularly risky. The challenge is in getting the data home, preferably by configuring a new data stream from the ORION bay to the *HST* science instrument data handling system. Like the ORION guiding functions, this issue requires further analysis.

Schedule. The Panel is well-aware that time is growing short for being able to select, construct, and test any new instrumentation for *HST* that would be launched in the FY09 time-frame. If an SM5 science instrument AO is to be issued, it should be done so as soon as possible. However, five years from selection to installation should be adequate, and is comparable to the development time for MIDEX or Discovery-class payloads.

3. SCIENCE PROGRAM

ORION observations will directly address science goals of the NASA Space Science Enterprise, including:

Origins:

- Investigate the origins of galaxies, stars, and planets.
- Understand how stars and planetary systems form and evolve.

SEU:

- Trace the life cycles of matter.
- Map the distribution of dark matter and the development of large scale structure.
- Determine the nature of dark energy and the history of cosmic expansion.

The discussion that follows is meant to indicate the potential scientific impact that an ultra-wide-field imager aboard *HST* would have, even if limited to a ~3-year mission. Other documents submitted to the Panel emphasize similar scientific themes, and there are many other fields that ORION could impact that we do not discuss.

3.1 Cosmology with ORION

Because the ORION field-of-view greatly exceeds those of WFPC2, ACS, and WFC3, while encompassing their collective wavelength coverage, ORION should be a powerful tool for cosmological problems, just as the previous *HST* cameras have been. ORION's large field, however, gives *HST* new power for several cosmological investigations that have been severely hampered by the small fields of previous cameras.

Dark Energy and Distant Supernovae

What is the nature of the dark energy? Does the expansion rate of the universe vary with time? At what redshift did the universe transi-

tion from being matter-dominated to being Λ -dominated?

The nature of the dark energy is perhaps the greatest mystery in modern physics. There is no shortage of ideas for candidates to explain dark energy, nor observational proposals to clarify its properties. The existence of dark energy was first revealed through supernova Type Ia (SN Ia) observations, however, and most critically, its plausible equations of state and their possible variations with cosmic time make clear and discriminatory predictions for what a richly observed SN Ia Hubble diagram will look like. The properties of the dark energy can be expressed in terms of its equation-of-state, $p/\rho c^2 = w$, that connects the energy density to the pressure. If the dark energy is a cosmological constant, then $w = -1$. For quintessence models, the equation of state is a function of redshift, $w(z)$, and its functional form depends on the form of the quintessential potential. If we parameterize $w(z) = w_0(z_0) + w'(z - z_0)$, then a precise SN Ia Hubble diagram, *with large redshift coverage*, can constrain w_0 and w' . *HST* has already been used to identify SN Ia at redshifts $z > 1$ where the Hubble expansion was truly still decelerating. NASA has recently called for studies of Dark Energy Probe mission concepts, some of which will advocate new spacecraft to obtain precise photometry of a large sample of SN Ia at all redshifts in order to generate diagnostic Hubble diagrams. The upshot is that the astronomical community can plausibly argue that significant resources should be devoted to the use of SN Ia as dark energy probes. Continuing to dedicate *HST* resources to this problem may provide a cost-effective and timely path both to refining the properties of dark energy and sharpening the approach of new investigations or space missions.

Ground-based SN Ia surveys first revealed the need for dark energy, and regardless of

what can be done in space, aggressive ground-based programs are already underway to refine at least the low-redshift SN Ia Hubble diagram. One such effort is the NOAO ESSENCE program to find and measure 200 SN Ia in the redshift range $0.15 < z < 0.7$; other SN Ia surveys will also commence, such as that to be done with the new CFHT Megacam. To completely explore the suite of dark energy candidates, however, requires SN Ia observations over the full range $0 < z < 1.7$ (Linder & Huterer 2003 Phys Rev D, 67, 081303; see **Figure 3.1**, taken from Tonry et al. 2003, ApJ, in press [astro-ph/0305008]). Disentangling w_0 from w' is only possible with a large redshift interval well beyond what can be sampled from the ground. These considerations are not trivial; while constant w has some appeal to simplicity, it cannot be forgotten that even that form was unanticipated a few years ago. Hard data on the expansion history at $z > 0.7$ is required how ever $w(z)$ is parameterized; the interval $z < 0.7$ is too limited to discriminate among the various dark energy candidates.

The ORION red/near-IR channel will be highly effective at observing SN Ia at $z > 0.5$. As SN Ia at yet higher z shift further into the near-IR, *HST*'s advantage over ground-based telescopes becomes increasingly large due to the bright atmosphere. In the *I*-band, *HST* will out-perform an 8-m class telescope for detecting isolated point sources, even in the best conditions; at the *J*-band the *HST* speed advantage exceeds 200. The Tonry et al. (2003) local SN Ia rate of $5.2 \times 10^{-5} \text{ Mpc}^{-3} \text{ yr}^{-1}$, for $\Omega_0=1$, $\Omega_\Lambda=0.7$, and $H_0=72$, implies that ~ 170 SN Ia within $0.5 < z < 1.7$ should be observed per square-degree per year, assuming that aside from time dilation, the supernovae rate does not evolve significantly with lookback time; for this cosmology the SN rate is nearly constant with redshift. Recent surveys with ACS actually give a high- z rate $2.5\times$ larger. For ORION, this translates to ~ 7 SN Ia yr^{-1} per field. Since the SN yield is directly proportional to the camera field, ORION is $\sim 6\times$

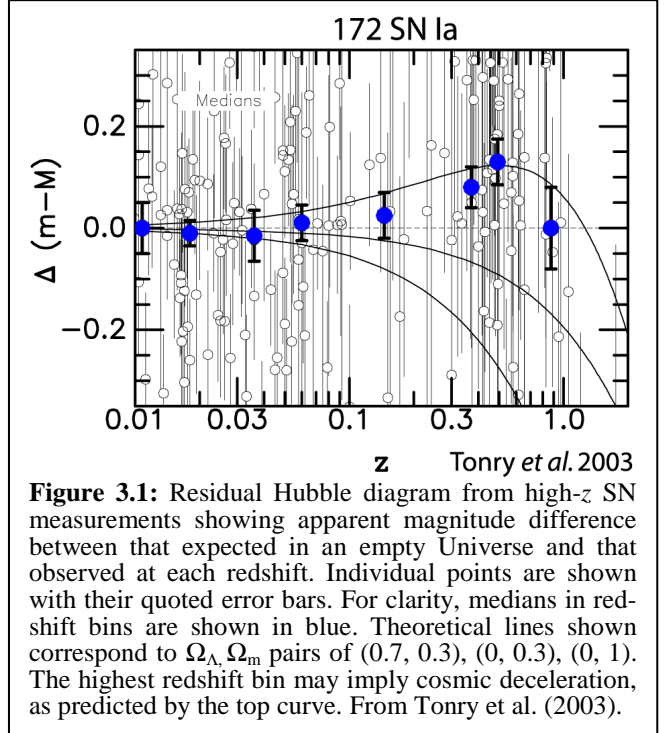


Figure 3.1: Residual Hubble diagram from high- z SN measurements showing apparent magnitude difference between that expected in an empty Universe and that observed at each redshift. Individual points are shown with their quoted error bars. For clarity, medians in redshift bins are shown in blue. Theoretical lines shown correspond to Ω_Λ, Ω_m pairs of (0.7, 0.3), (0, 0.3), (0, 1). The highest redshift bin may imply cosmic deceleration, as predicted by the top curve. From Tonry et al. (2003).

faster than ACS/WFC (which has no NIR channel in any case), $\sim 8\times$ faster than WFC3/UVIS, and $\sim 12\times$ faster the WFC3/IR. A weekly cadence (exploiting the time dilation for high- z SN) of hour-long exposures in four bands (2 optical/2 near-IR) suggests a yearly investment of ~ 100 hours for 7 SN Ia. Spending ~ 1000 hours of *HST* time in each of 3 years could readily generate a sample of ~ 210 SN Ia events at $z > 0.5$. If this sample is combined with ground-based data at $z < 0.7$, then this would complete a Hubble diagram accurate to $< 5\%$ on $\Delta z = 0.1$ scales. Accuracy of this sort will be sufficient to find any large surprises in the expansion history of the universe at the epochs at which deceleration is assumed to occur, and would set the stage for a future Dark Energy Probe mission that will sample several thousand SN Ia.

Dark Matter and Lensing

How is dark matter distributed? How does dark matter cluster through cosmic time?

The “weak lensing” of distant galaxies by large-scale inhomogeneities in the foreground distribution of mass has long been advocated as a means to probe the mass perturbation power-spectrum of the universe. It is also a means to track the growth in amplitude of those perturbations as the last scale structure of the universe grows and evolves. Large-format ground-based cameras in the optical have been used or are being advocated to probe weak lensing at $z < 1$; however the bright near-IR sky makes it exceedingly difficult to extend this work to higher redshifts. The dual-channel ORION camera, however, should be extremely powerful for lensing studies over a wide range of redshifts. The large wavelength coverage of ORION plus its dichroic make it an effective engine for producing galaxy photometric redshifts, particularly for galaxies at $z > 1$. ORION imagery of ground-based lensing survey fields thus enhances isolation of the lensing signature by allowing for the background and foreground objects to be identified at all redshifts, leading directly to a characterization of the mass power-spectrum as a function of redshift.

Apart from ground-based work, however, the combination of high spatial resolution over large angular scales afforded by ORION should lead to better isolation of the lensing signal, at least on the smaller scales being probed by ground-based instruments. The novel use of ORION, however, will be in probing the power-spectrum at $z > 1$, something that is presently not possible (via weak lensing) with any existing instrument. ORION can thus serve as a direct and unique witness to the growth of structure at $z > 1$.

The Early Universe

How are galaxies assembled in the early universe? What do morphologies and colors reveal about the proto-galaxy merger history? Can we penetrate the $z > 5$ universe?

The *JWST* will be superb for exploring the early history of the universe at $z > 5$, yet *HST* with WFPC2, ACS, and NICMOS is already making important contributions to observing the first stages of galaxy formation. The *JWST* NIRCcam FOV is 10.6 sq-arcmin, similar to that of the ACS/WFC, and it is twice as large as the field of the WFC3 near-IR channel. Given that the speed of *JWST* vs. *HST* goes like the fourth-power of aperture diameter (for diffraction-limited but sky-dominated imagery), it is exceedingly expensive to survey any large area with *HST* at flux levels relevant to most *JWST* early universe studies. The ORION field coupled with the dichroic closes this gap by an order of magnitude, and would thus allow *HST* to serve as an effective *JWST* pathfinder.

Theoretical studies show that the brighter portion of the proto-galaxy population should be readily visible at integrated fluxes of 10 nJy. *HST*+ORION should be able to reach this flux for point sources at the 5σ level in 24 hours. If we allocate 50 hours per band to allow for better limits on the *non*-detection of objects, making use of the dichroic gives a 200 hr investment to survey each ORION field to 10 nJy in eight bands (UV $_{ubv}$ /ri zJ). Significantly, the combination of the ORION optical and near-IR channels will be highly effective at isolating galaxies at $z > 5$ by identifying the Ly α -break.

At this writing, it does not appear that the science goals of the *JWST* design reference mission (DRM) have fully incorporated the implications of *JWST*’s lack of coverage in the optical, coupled with the specification that it will only be diffraction-limited at 2 μ m. *JWST* imagery coupled with deep optical/near-IR ORION data will cleanly separate $z > 5$ proto-galaxies from objects at lower redshifts, and accurate photometric redshifts for at least the brightest of the objects at $5 < z < 10$.

The large field of ORION offers two additional scientific augmentations of the *JWST* DRM. First, narrow-angle, deep “blank-sky” surveys, which are likely to be common to *JWST* work, are always vulnerable to cosmic variance. ORION imagery at least allows the context of narrower *JWST* surveys to be understood as it can be characterized by the brighter objects at $z > 5$. Finally, ORION offers the opportunity to find the rarest and brightest objects at $z > 5$ that may be absent in single NIRCам fields. In short, *HST*+ORION offers a complementary wide but shallow (10 nJy) precursor survey to the forthcoming narrow and deep (1 nJy) *JWST* surveys.

3.2 Star Formation with ORION

Star formation is the fundamental process that determines the fate of baryons in the universe. ORION observations can be used to build a better understanding of star formation, the implications for the chemical and dynamical evolution of galaxies and the formation of planetary systems, and, ultimately, the rate at which baryonic matter is locked away into long-lasting repositories and removed from cosmic recycling.

As the total mass of material involved in the star formation process increases, the maximum stellar mass formed in these regions also increases. Because the amount of ionizing radiation grows dramatically with slight changes in effective temperature (and therefore stellar mass), the degree to which H II regions affect the dynamics of their parent dark clouds differs between the smallest star forming regions and the largest ones. There are other natural physical scales to star formation, including the importance of magnetic pressure support within collapsing clouds, clustering, triggering, and the coherence length of the process relative to the size of the galaxy. Additional global characteristics of star formation that are largely unexplored, but which a well-designed survey could address,

include the frequency of disks within different kinds of H II regions, morphological types of ionized structures, and the feedback role of winds, shocks, bubbles, mergers, and Herbig-Haro jets in different types of star forming regions.

Physical Classification of Star Formation

Does star formation occur in discrete, hierarchical units? What physical thresholds determine the nature of star forming regions?

Probing the physics of star formation is a multi-wavelength endeavor; observations from X-ray through radio wavelengths contribute complementary information on the stellar, gaseous, and dusty components involved. Short wavelength observations diagnose massive stars and energetic processes such as accretion and shock waves driven by hypersonic jets ejected from young stellar objects (YSOs). Long wavelength observations penetrate extinction to reveal embedded nascent sources, low-mass objects, and circumstellar disks.

One way to improve our understanding of star formation, in light of the multitude of observational techniques across the entire electromagnetic spectrum, is to form a structure for grouping similar objects together in order to isolate the major physical processes at work over different size and mass scales. In **Table 3.1** we provide a preliminary hierarchical classification scheme for star forming regions, organized from the smallest and least massive to the largest and most massive. As expected, we currently know the most about the closest (and smallest) regions of star formation. Analogous to the extragalactic distance ladder, we hope to apply what we learn about nearby regions of star formation to understand those far away.

ORION can be used to survey a large sample of star forming regions in the Solar neighborhood and in nearby galaxies to bring together a coherent dataset using the same diagnostic filters for determining common or

Table 3.1: Hierarchical Star Formation Classification

Type	Example	Description
B	Bok Globule	Isolated activity in a single, distinct cloud core that makes a single or binary star.
T	Taurus-Auriga	A loose collection of dark clouds that forms exclusively low-mass stars. The most massive star that forms is later than $\sim B3$, so there are no significant H II regions that influence the cloud dynamics, even when the region is young. A typical region forms several dozen, up to ~ 200 stars.
P	Perseus	A star forming region with early B stars but no O stars. A few small clusters form, and there are small H II regions within young regions of this type. All star formation remains subcritical; that is, ambipolar diffusion of magnetic fields from cloud cores enables a gradual collapse as star formation begins. Several hundred stars form.
O	Orion	The first late O-stars appear, and the H II regions limit the lifetimes of disks around low mass-stars in the area by photoevaporation (i.e., proplyds exist). Significant clustering occurs, and thousands of stars form in the most massive cluster. Supercritical star formation, where magnetic fields are dragged into the collapsing molecular cloud cores along with the infalling gas, is the dominant mode of star formation. Supernovae begin to play a role in the dynamics over the lifetime of the cloud, which may show evidence for propagating episodes of star forming activity.
C	Carina	The most massive stars allowed by the Eddington limit form. Winds from these supernova progenitors dissipate the cloud.
D	30 Doradus	More than a couple dozen Wolf-Rayet stars evolve. A single, massive cluster dominates the dynamics of the region.
G	Giant H II Region	Several 30-Doradus-like regions exist, and they physically overlap one another. Galactic rotation plays a role in limiting the extent of the star forming region. There is a specific coherence length to the process; that is, a plot of age differences against physical distance shows a turnover at some characteristic length scale.
M	Mergers	Star formation processes that only occur when galaxies merge. The coherence length is unlimited. Super-star clusters, analogs of young globular clusters, form in these systems.

disparate characteristics that may depend on environment, metallicity, or dynamical interaction history. This large dataset can be used to probe coherence lengths and correlations between stellar and emission-line luminosities. In particular, we concentrate on high-mass star forming regions since (a) these are the sites where most stars form, and (b) these are the regions that we observe at high redshift but cannot resolve in detail. This second point is salient, for it stresses the importance of UV/optical investigations in the local universe because this is the light which is redshifted to infrared wavelengths in the most distant objects to be studied by *JWST*. In many ways, *JWST*'s study of the early universe is a

UV/optical science investigation performed at infrared wavelengths.

The Nearest Star Formation/Planet-Forming Regions

How do stars form and what determines their masses? How does star formation self-regulate? How common are planetary systems?

HST's sub-arcsecond images have revolutionized our understanding of the early phases of stellar and protoplanetary disk evolution, the properties of protostellar jets and their interactions with their surroundings, and the hazards of intense radiation fields to planet

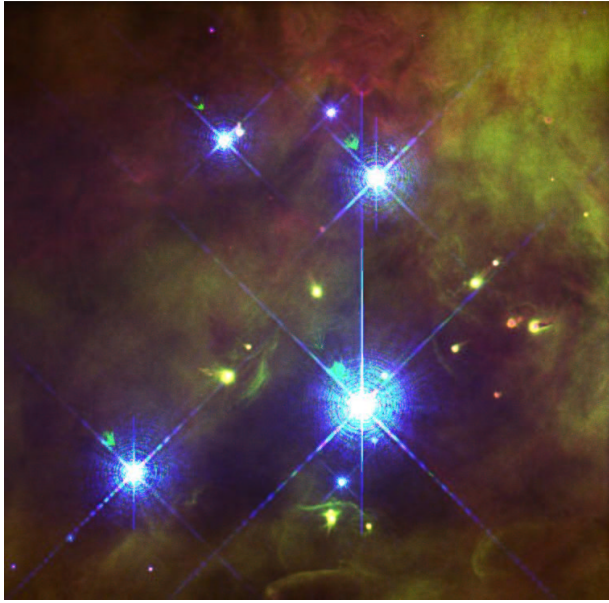


Figure 3.2: (top) The central portion of the Orion Nebula cluster showing the Trapezium stars along with about a dozen photo-evaporating protoplanetary disks. (bottom) A silhouette disk in a binary system embedded within the HII region M43. Note the distortions in the disk, and the bipolar jet that emerges from its center. Though extensively studied from the ground, the true nature of such objects in M42/43 was not revealed until imaged by *HST*.

formation. For example, while mature planetary systems are very hard to detect and characterize, forming systems are directly observable in the nearest star forming regions (**Figure 3.2**). *HST* has shown that protoplanetary disks embedded in HII regions such as the Orion nebula (“proplyds”) are rapidly de-

stroyed by the UV radiation emitted by nearby massive stars. But there are additional hazards to forming planetary systems — processes which may play fundamental roles in setting the masses, multiplicity, and clustering properties of stars.

The Orion nebula is typical of the type of environment in which most stars (both high and low mass) are born. Because most stars form from giant molecular clouds, dark clouds (such as Taurus) produce only a few percent of all stars. Regions such as Orion, which spawn thousands at once, produce the vast majority. *HST* imaging surveys of YSOs in the nearest regions of active star formation are therefore among the most important probes of star and planet formation in general.

There are several dozen giant molecular clouds/H II region complexes within several kpc of the Sun, a region where *HST*-ORION’s 0.1” resolution can detect and characterize proto-solar system sized objects, resolve stellar multiplicity, and map the cores of forming star clusters. These regions include M16, M17, and the Carina nebula, which produce 100 times the UV radiation generated by the massive stars in the Orion nebula. So far, only the Orion nebula has been mapped in detail by *HST*; it harbors the highest concentration of exposed protoplanetary disks known, discovered by optical *HST* imagery, which has proven to be a remarkably efficient technique. With the ORION camera, we can extend these detailed studies to more distant and larger high-mass star forming regions in order to conduct a census of protoplanetary systems as a function of star forming class.

Recent studies of star forming regions have shown that the majority of stars are born in close proximity to massive stars that produce torrents of UV radiation, and that most stars form in very dense (but short-lived) clusters. Not only do protoplanetary disks have to survive intense heating by UV radiation during the first 1 to 30 million years of their existence (**Figure 3.3**), but they are also exposed

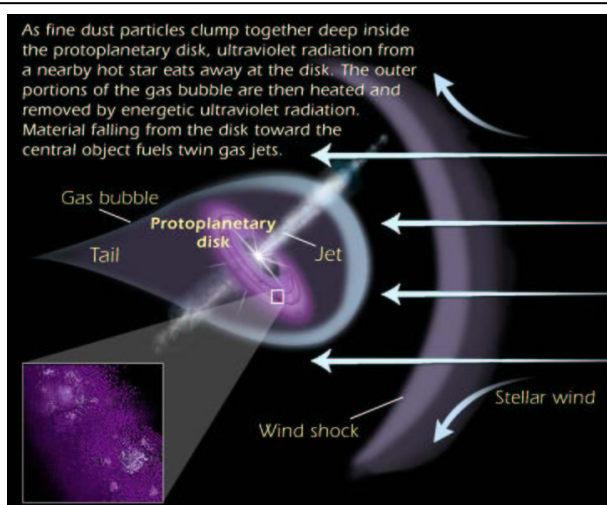


Figure 3.3: Protoplanetary disks in high-mass star-forming regions are exposed to intense UV radiation fields and winds from massive stars. Disks must be able to survive within such environments if planetary systems are common.

to disk and envelope truncating passages of sibling stars, the impacts of protostellar outflows, massive star winds, and supernova explosions. Such dynamical interactions, UV radiation, and mass flows can profoundly affect the star-forming environment. Destruction of cloud cores, star-forming envelopes, and the disks by interactions with other protostars, young stars, or more mature siblings may regulate the mass available to a star and its planetary system.

We do not yet understand the full impact of UV radiation, dynamical hazards, or the effects of mass flows on the stellar and planetary birthing process. Advancing our understanding requires complete surveys of entire star-forming complexes and a global systems approach to the process by which interstellar matter is converted into stars and planets. For example, in Orion, active star formation extends over the 10 square-degree area of the Orion A and B molecular clouds. This extended region has only recently been completely imaged with modern CCD mosaics from the ground. However, these data lack the resolution to directly detect disks. Yet evidence for disks is inferred from IR excess, $H\alpha$

emission, and jets and outflows identified with narrow-band filters. Indeed, where *HST* has observed, it tends to reveal, in a single ACS field, multiple disks or evidence of embedded sources and dozens of shock structures from criss-crossing flows.

Young stars and circumstellar disks in the extended Orion region experience much less external radiation than those located in the highly-irradiated core of the nebula. However, in more virulent star-forming regions such as Carina, hazards to planet formation may be orders of magnitude greater than in the relatively benign outer reaches of Orion. A large-scale survey of Orion, Carina, and other regions within ~ 2.5 kpc of the Sun would address the following goals:

- Determine what fraction of disks survive [1] disk truncation by dynamical processes, and [2] photo-ablation by UV radiation fields as a function of distance from the most massive stars.
- Determine how the environment affects the masses of stars and the IMF.
- Infer how rapidly planets can form in surviving disks, and what the grain properties are. (Do grains grow rapidly? What role do disk instabilities play? Do they lead to rapid giant-planet formation, or merely fuel accretion onto stars?)
- Map the structure of outflows to provide a fossil record of protostellar accretion activity and environmental effects. Jet morphologies provide evidence for disk precession or interactions with side-winds. (Precession generates S-shaped outflows; sibling encounters produce Z-shaped flows; relative motion between the source and surrounding medium leads to C-shaped flows.)
- Probe nebular and shock dynamics. Provide a legacy of high-resolution images which in the future can be used to measure

additional motions for gauging energy and momentum feedback to the parent cloud.

Applying our Local Knowledge Outward

Are the physical processes observed in nearby H II regions also observed in star forming regions in external galaxies? How is massive star formation triggered in nearby galaxies? What are the ultimate size and mass limits to massive star forming clusters?

Extending the H α imaging / H II region classification scheme (derived from B through C in Table 1) to nearby galaxies (D through M) will enable us to study these star formation processes over a much more diverse range of absolute star formation rates (SFRs) and physical conditions in the ISM (**Figure 3.4**). For example, within 10 Mpc we can probe regions varying in metal abundance from 1/40 to 2-3 times solar, cold gas column densities ranging from 10^{19} to 10^{24} cm $^{-2}$ (and a comparable dynamic range in ISM pressures), and star forming clusters ranging in mass from < 100 solar masses to 10^5 solar masses (e.g.,

Kennicutt 1998, ARAA, 36, 189). An enormous body of multiwavelength observations will be available from the SIRTf Nearby Galaxies Survey (SINGS: Kennicutt et al. 2003, PASP, in press) and other smaller scale surveys. The ORION camera would add the critical element of high-resolution UV, visible, and near-IR imaging of these regions in H α and the stellar continuum, sufficient to resolve the individual star-forming regions and clusters over this full physical parameter space.

One of the most powerful diagnostics of the structure and clustering properties of star formation is the H II region luminosity function (HIILF; Kennicutt et al. 1989, ApJ, 337, 761; Thilker et al. 2002, AJ, 124, 3118; and references therein). For regions ionized by large numbers of OB stars the HIILF directly traces the mass spectrum of the ionizing OB associations or star clusters. Ground-based studies have shown that the form of the clustering spectrum is a strong function of galaxy type, and varies systematically in different ISM environments, for example in spiral arms as compared to the general disk environment (Kennicutt et al. 1989; Oey et al. 2003, AJ, in

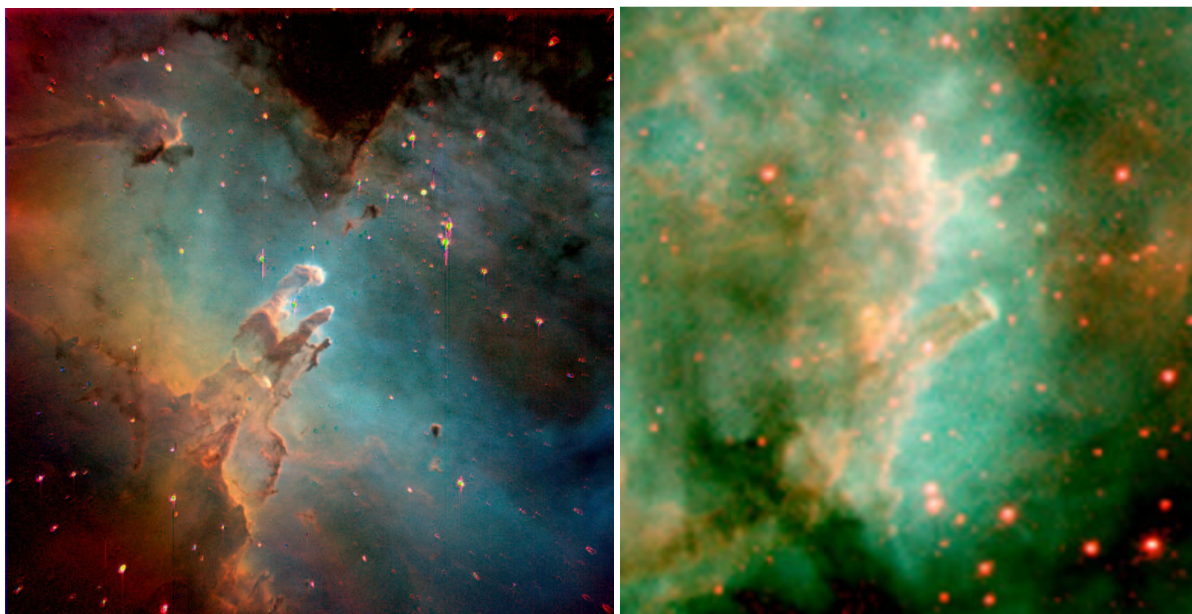


Figure 3.4: Comparable structures are seen in the Eagle Nebula (*left*) and 30 Doradus (*right*). Analysis of the microphysics in the Eagle Nebula allowed direct analysis of the dynamics at work in 30 Doradus by applying the physics learned to a system where such physical resolution was impossible (Scowen et al. 1998, AJ, 116, 163).

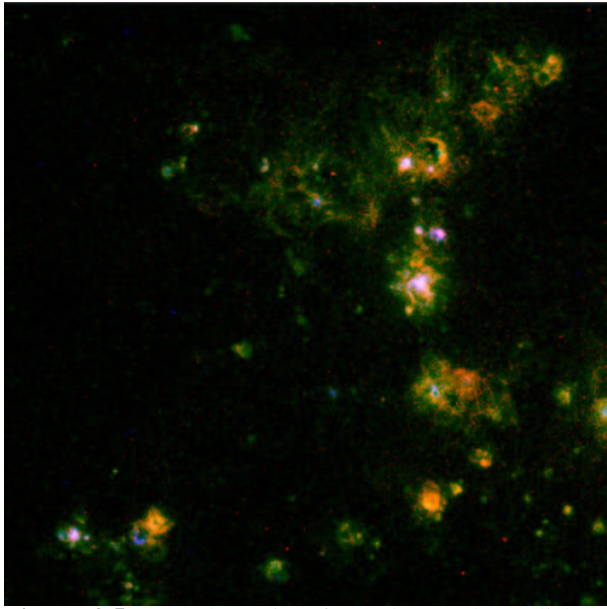


Figure 3.5: Sample region from the southern disk of M101 observed at $0.1''$ resolution with WFPC2. This field shows regions of star formation in $H\alpha$, [O III], and [S II] emission. We can tie the underlying physical properties of nearby examples studied at far higher resolution to the integrated properties of the various regions.

press) though the physical mechanisms driving this variation are not yet clear. *HST* observations of the HIILF in M51 by Scoville et al. (2001, AJ, 122, 3017) have demonstrated the importance of high spatial resolution for resolving the H II regions and accurately measuring the form of the luminosity function.

Independent information on the mass spectra of young clusters in galaxies will come from UV to infrared broad-band imaging of these clusters. Observations of interacting and merging galaxies with *HST* have revealed a new class of “super star clusters” (SSCs) and the suggestion that massive globular clusters are being formed in many galactic mergers (e.g., Whitmore et al. 1999, AJ, 118, 1551). What remains unclear is whether the present-day formation of globular clusters is limited to these violent merging environments, or whether instead such clusters are a natural consequence of star formation in large gas-rich galaxies. This question can only be addressed with high-resolution observations of

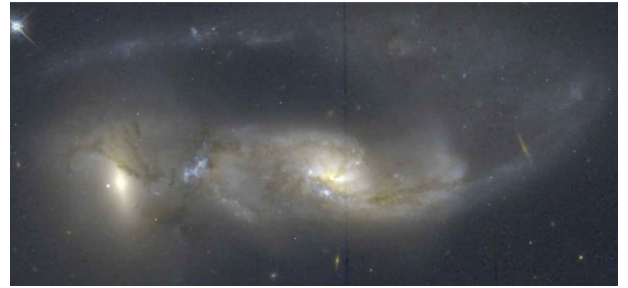


Figure 3.6: Color image of NGC 6621/2 showing the SSC population triggered by the massive interaction/merger event occurring between the two galaxies.

nearby galaxies — with sufficient linear resolution to unambiguously identify young, gravitationally bound clusters — with wide wavelength and spatial coverage to accurately measure the stellar masses and ages of these clusters and the associated ionized gas structure and luminosities over a wide range of galactic environments. **Figure 3.5** demonstrates the potential for achieving these goals at 5 Mpc distance with $0.1''$ imaging.

Recent work by Keel & Borne (2003, astro-ph/0307025) on the observed properties of SSCs in dynamically interacting galaxies has yielded the following intriguing trends: (1) The colors and apparent ages of SSCs seem to form a continuum and are correlated with the “age” of the dynamical encounter (i.e., time since closest approach between the two galaxies). (2) SSCs are much brighter than ordinary clusters ($M_V = -14$) but comparable to globular clusters (GC). An important issue is whether these are indeed the progenitors of GCs, since they have a power law LF like ordinary star clusters (not the gaussian LF of GCs), but the photometric evolution of these systems is unclear and in need of more observational work. (3) Currently most SSC studies are in merger events (Antennae galaxy, etc.), but Keel & Borne make the (strong) point that we need studies of SSC properties in various stages of dynamical interaction. The image of NGC 6621/2 (**Figure 3.6**) is their example of a recent strong tidal encounter. The bright blue SSC between these galaxies is accompanied

by strong kinematic perturbations that imply that a dynamic interaction threshold is what drives whether SSCs form.

Based on these observations, we would want to study properties of SSCs at $0.1''$ resolution, with sufficient UV sensitivity. Our sample needs to include many interacting systems (i.e., mass ratios and closest approach values) to determine what drives the number and brightnesses of the triggered SSCs. These could represent a unique mode of star formation *and* they may be the progenitors of a component of the stellar populations in galaxies whose origin has been a long-standing puzzle (the GCs).

Star formation survey. A comprehensive survey of Galactic, LMC/SMC, and nearby galaxy star forming regions and SSCs will utilize the complete suite of ORION filters. This exciting set of high-resolution images will comprise the first consistent, panchromatic imaging survey of its kind. The UV to *H*-band broad filters will characterize the stellar components. The narrow-band filters (Mg II, [O II], H β , [O III], H α , [S II], and [Fe II]) will cover a large range of physical conditions (temperatures, densities) and will distinguish photoionized and shock-excited features. Spending 4 orbits per pointing, in 1800 orbits (600 in each of 3 years) the survey would cover 7.5 sq-degrees, sufficient to sample the main structures of a dozen Galactic H II regions of various classes, several square degrees in the Magellanic Clouds, and ~ 30 external galaxies of diverse properties.

4. MIDEX IMPLEMENTATION

The science return from ORION or a similar instrument aboard *HST* would be truly phenomenal. The data volume and sky coverage in a three-year mission would exceed any previous instrument and would provide researchers with a treasure-trove of data to mine long after *HST* operations cease. For certain science programs — especially those that probe the high-redshift universe and rely on good

sensitivity, or require high-resolution imaging or spectroscopic follow-up — substantive progress may only be made in the ~ 2009 timeframe via *HST* instrumentation. Nevertheless, a large fraction of the imaging survey science included here could be accomplished by a MIDEX-class mission.

Almost all of the observing programs described here require a spatial resolution of $\sim 0.1''$ at optical wavelengths to achieve the science goals. Higher spatial resolution, such as that available with *HST*-ACS or WFC3, would be better for some programs, but the outstanding and lengthy track record of *HST*-WFPC2 imaging with $0.1''/\text{pixel}$ has shown that important physical scales can be distinguished at this imaging resolution. Choosing $\sim 0.1''/\text{pixel}$ for ORION aboard *HST* is a compromise between providing satisfactory spatial resolution (which can be enhanced by employing dithering techniques) while achieving a very wide FOV using a reasonable number of detectors, even though this scale undersamples the *HST* diffraction limit in the UV/optical ($0.057''$ at V, Rayleigh criterion).

An ORION-like imager could achieve similar resolution performance if it were implemented on a 1.2-meter MIDEX-class mission (diffraction limit = $0.115''$ at V, Rayleigh criterion).¹ Ideally, the mission would operate in an earth-Sun L2 orbit, allowing for greater observing efficiency compared to a low-earth orbit mission such as *HST*. In addition, a somewhat larger FOV can be contemplated that would increase the sky coverage of a dedicated mission.

Assuming identical instrumentation, the speed of a 1.2-meter class wide-field imaging telescope would be at least 4 times slower than *HST*, depending on the nature of the target. For this reason, a MIDEX implementation

¹ The lead author and a subset of the contributors are in parallel developing a MIDEX version of ORION to be proposed in the next MIDEX round currently scheduled for May 2004, with launch in 2010 or 2011.

is probably not advisable in lieu of a larger Dark Energy Probe mission to investigate the history of cosmic expansion and the nature of dark energy to high precision using distant (i.e., faint) SN Ia's. However, at L2, a highly efficient, dedicated survey of star forming regions could be undertaken to cover 15-20 sq-degrees per year. We estimate that >30 Galactic HII regions, half of the LMC, and several dozen nearby galaxies could be surveyed in multiple bandpasses with $\sim 0.1''$ resolution in a three-year mission. An extended mission could also impact large-scale structure and galaxy evolution studies, and could be used in conjunction with *JWST* to achieve UV to mid-IR observations of a wide variety of targets; the MIDEX observations at $\sim 3800\text{\AA}$ would match the resolution of *JWST* at 2 microns (but would be ~ 600 times slower at detecting faint point sources in sky-dominated observations).

To enact such a mission using only US government and industry resources (i.e., no foreign participation) we estimate could require a budget of $\sim \$250\text{M}$ or possibly more (including the mandatory 20% budget reserves). Compared to the cost of a Hubble servicing mission plus a new instrument, a MIDEX implementation may represent a more cost-effective approach to achieving an ultra-wide-field UV/optical imaging capability from space. However, we note the following: (1) An *HST* imager is likely to have a broader scientific impact than a focused MIDEX mission, even if post-SM5 operations were of shorter duration, due to the large collecting area of *HST*, broad community access, and opportunities for follow-up high-resolution imaging and spectroscopic observations. (2) SM5 would nominally occur 1-2 years sooner than a MIDEX could be developed and launched. On the one hand, the *HST* data would already have impacted numerous fields of study by the time the MIDEX could launch, while generat-

ing mountains of data that would be available in the *HST* archive for Cycle 1 *JWST* observers to cull. On the other hand, the MIDEX mission could operate at very low additional cost well into the *JWST* era, while it appears that *HST* operations would be terminated no later than ~ 1 year after *JWST* launches. (3) It is not clear that the budget for the next round of MIDEX missions is sufficient to support a truly panchromatic, wide-field imaging mission as considered here, nor is it by any means certain that such a mission would be selected for flight from among the anticipated 35-40 proposals that will be submitted. (4) Finally, it must be remembered that a simple cost-benefit and schedule analysis is not sufficient for judging the relative merits of an *HST* versus MIDEX implementation. We can be sure that either implementation would resonate positively with the taxpaying public since the data product will be spectacular, both scientifically and aesthetically. However, implicit in this discussion is that an SM5 mission poses a tangible danger to human life, whereas a MIDEX mission minimizes such considerations. Nevertheless, the proven track record of previous *HST* servicing missions suggests that deploying new instrumentation such as ORION can be successful and result in a very high science return.

Acknowledgements

The authors wish to thank scientists and engineers at STScI, the HST Project at NASA-GSFC, and Rockwell Scientific for their aid in developing this description of the ORION concept. In particular, JM thanks Ed Nelan for useful discussions concerning *HST* guiding; Pam Sullivan and Craig Tooley for technical advice; Dave Leckrone for insights on the scientific program; and James Garnett and Yibin Bai for information on detector technologies.